Cholesterol modulates the recruitment of Kv1.5 channels from Rab11-associated recycling endosome in native atrial myocytes

Elise Balse[a,b], Saïd El-Haou[a,b], Gilles Dillanian[a,b], Aurélien Dauphin[c], Jodene Eldstrom[d], David Fedida[d], Alain Coulombe[a,b], and Stéphane N. Hatem[a,b,1]

[a]Institut National de la Santé et de la Recherche Médicale, Unité Mixte de Recherche Scientifique-956, 75013 Paris, France; [b]Université Pierre et Marie Curie, Paris-6, Unité Mixte de Recherche Scientifique-956, 75013 Paris, France; [c]Plate-forme imagerie cellulaire IFR14, 75013 Paris, France; and [d]Department of Anesthesiology, Pharmacology and Therapeutics, University of British Columbia, Vancouver, BC, Canada V6T 1Z3

Edited by Lily Y. Jan, University of California, San Francisco, CA, and approved June 19, 2009 (received for review March 17, 2009)

Cholesterol is an important determinant of cardiac electrical properties. However, underlying mechanisms are still poorly understood. Here, we examine the hypothesis that cholesterol modulates the turnover of voltage-gated potassium channels based on previous observations showing that depletion of membrane cholesterol increases the atrial repolarizing current I_{Kur}. Whole-cell currents and single-channel activity were recorded in rat adult atrial myocytes (AAM) or after transduction with hKv1.5-EGFP. Channel mobility and expression were studied using fluorescence recovery after photobleaching (FRAP) and 3-dimensional microscopy. In both native and transduced-AAMs, the cholesterol-depleting agent MβCD induced a delayed (≈7 min) increase in I_{Kur}; the cholesterol donor LDL had an opposite effect. Single-channel recordings revealed an increased number of active Kv1.5 channels upon MβCD application. Whole-cell recordings indicated that this increase was not dependent on new synthesis but on trafficking of existing pools of intracellular channels whose exocytosis could be blocked by both *N*-ethylmaleimide and nonhydrolyzable GTP analogues. Rab11 was found to coimmunoprecipitate with hKv1.5-EGFP channels and transfection with Rab11 dominant negative (DN) but not Rab4 DN prevented the MβCD-induced I_{Kur} increase. Three-dimensional microscopy showed a decrease in colocalization of Kv1.5 and Rab11 in MβCD-treated AAM. These results suggest that cholesterol regulates Kv1.5 channel expression by modulating its trafficking through the Rab11-associated recycling endosome. Therefore, this compartment provides a submembrane pool of channels readily available for recruitment into the sarcolemma of myocytes. This process could be a major mechanism for the tuning of cardiac electrical properties and might contribute to the understanding of cardiac effects of lipid-lowering drugs.

cardiac myocytes | ion channels | membrane lipids | trafficking | channel recycling

Lipids are important determinants of cardiac excitability. For instance, free cholesterol is a major lipid class that regulates fluidity, curvature, and stiffness of cellular membranes (1). In addition, cholesterol can modulate the function of a number of cardiac ion currents through effects on channel properties (2, 3). There is also recent clinical and experimental evidence that lipid-lowering therapy, such as statins, exert anti-arrhythmic effects. However, these pharmacological effects of statins are poorly understood and could involve their pleiotropic effects as well as the reduction of the cholesterol content of cardiac membranes (4, 5). Hence, better understanding of mechanisms responsible for cholesterol effects on cardiac electrical properties is of major interest from both a fundamental and clinical point-of-view.

In cardiomyocytes as in other excitable cells, the surface density of functional channels is a dynamically regulated process and results from a balance between endocytic and exocytic trafficking processes. For instance, the inhibition of the motor protein dynein increases potassium current by preventing the retrograde trafficking of Kv channels in cardiomyocytes (6, 7). Recycling has an important role in the regulation of expression of KCNQ1/KCNE1, pacemaker HCN channels and Kv1.5 channels. This process involves several Rab-GTPases (8–10). Rab-GTPases regulate the trafficking of vesicles between plasma membrane and intracellular compartments by regulating sorting, tethering and docking of trafficking vesicles. Rab4, associated with the early endosome (EE), mediates the fast recycling process while Rab11, linked to the recycling endosome (RE), is involved in slow recycling of proteins back to the cell surface. However, the role of ion channel turnover in cardiac excitability still remains to be investigated.

Previous studies have reported that membrane cholesterol can modulate the surface expression of potassium channels (11–13). For instance, in neonatal rat myocytes, cholesterol depletion causes a fast redistribution of Kv1.5 channels at the plasma membrane (12). Kv1.5 channels are the molecular basis of the main repolarizing current of the atria, I_{Kur} which is involved in the pathophysiology of atrial fibrillation (14). Here, we hypothesized that cholesterol depletion and increased membrane translocation of Kv1.5 channels may underlie the increased I_{Kur} (12). Cholesterol can also act on different stages of the recycling process in various cell types (15–19).

In this study, trafficking and functional expression of Kv1.5 channels were investigated in rat adult atrial myocytes (AAM). Using single-channel recordings, high spatial resolution 3D-microscopy and fluorescence recovery after photobleaching (FRAP), we identified a submembrane pool of Kv channels available for recruitment into the plasma membrane of myocytes upon cholesterol depletion.

Results

Cholesterol Content Regulates Potassium Currents in Myocytes. Perfusion of 1% MβCD caused a drastic increase in the amplitude of the sustained outward potassium current, I_{Kur}, in AAM overexpressing EGFP-tagged Kv1.5 channels (at + 60 mV: 21.6 ± 5.3 pA/pF before MβCD vs. 62.5 ± 10.8 pA/pF upon MβCD, $n = 11$, $P < 0.001$) (Fig. 1). This effect occurred at a fixed time of 6–10 min after drug application. Low concentrations of 4-AP (500 μmol/L) inhibited most of the MβCD-induced current indicating that it was mainly underlain by Kv1.5 channels (Fig. 1 *A* and *B*).

In native (nontransduced) myocytes too, 6–10 min of MβCD

Author contributions: E.B., A.C., and S.N.H. designed research; E.B., S.E.-H., G.D., and A.C. performed research; A.D., J.E., and D.F. contributed new reagents/analytic tools; E.B., S.E.-H., A.C., and S.N.H. analyzed data; and E.B., J.E., D.F., A.C., and S.N.H. wrote the paper.

The authors declare no conflict of interest.

This article is a PNAS Direct Submission.

Freely available online through the PNAS open access option.

[1]To whom correspondence should be addressed at: Unité Mixte de Recherche Scientifique-956, Faculté de Médecine Pierre et Marie Curie, Paris-6, 91 boulevard de l'Hôpital, 75013 Paris, France. E-mail: stephane.hatem@upmc.fr.

This article contains supporting information online at www.pnas.org/cgi/content/full/0902809106/DCSupplemental.

PHYSIOLOGY

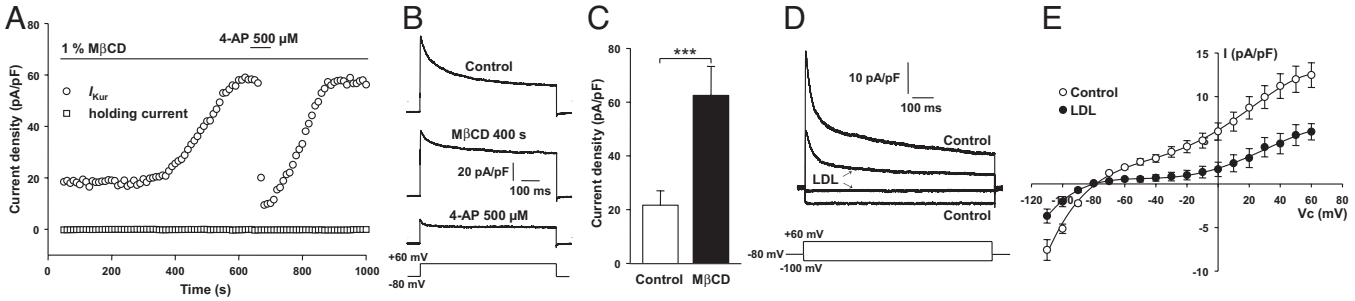

Fig. 1. Effect of cholesterol on potassium currents in adult atrial myocytes. (*A*) Time courses of the effect of 1% MβCD and 500 µM 4-AP perfusions on I_{Kur} and holding current measured in hKv1.5-EGFP transduced AAM. (*B*) Traces of currents recorded in Tyrode, at steady state effect of 1% MβCD and of 4-AP. (*C*) I_{Kur} densities measured in control Tyrode and MβCD (n = 11). (*D*) Superimposed traces of inward background and outward currents recorded in control and in LDL-treated myocytes. (*E*) Current-voltage curves in control (n = 11) and LDL-treated (n = 11) myocytes.

application increased I_{Kur}, an effect blocked by 500 µmol/L 4-AP (8.4 ± 2.4 pA/pF before MβCD vs. 43.0 ± 5.8 pA/pF upon MβCD, $n = 4$, $P < 0.01$). Two time-dependent components of the outward current could be analyzed using a biexponential function to identify fast and slow components that correspond to different channel populations (20). Interestingly, the fast component most likely corresponding to Kv4.x channels was decreased from 16.4 ± 4.0 to 8.6 ± 1.4 pA/pF without any change in its time-dependent inactivation (τ_{fast} control: 24.7 ± 2.9 s; τ_{fast} MβCD: 20.4 ± 3.4 s; $n = 7$). As control experiments, AAM were perfused with a mixture of cholesterol and MβCD in an 8:2 ratio that did not stimulate I_{Kur} in either native or transduced myocytes, as previously described (12).

To further examine the role of cholesterol in the regulation of potassium currents, native AAM were incubated for 24 h with 50 µg/mL low density lipoprotein (LDL), used as a cholesterol donor. LDL reduced both the sustained outward potassium current and the inward rectifying potassium current, I_{K1} (Fig. 1 *D* and *E*; n = 11 for both control and MβCD), as described in vascular cells (21). These results indicated that cholesterol content regulates the density of cardiac potassium currents and that I_{Kur} is particularly sensitive to this regulation.

MβCD Increases the Density of Functional Kv1.5 Channels in Myocytes. Single-channel recording was used to examine directly whether cholesterol depletion increased the number of Kv1.5 channels in the plasma membrane. In freshly isolated AAM (Fig. 2*A*), upward openings of potassium channels were observed under control conditions (mean current from channel openings: 1.4 ± 0.4 pA, n = 10 patches) with an elementary conductance of 11.8 ± 1.5 pS. After approximately 6–10 min of MβCD application, a marked increase in channel activity occurred and reached a high mean value (35.2 ± 5.5 pA, $n = 10$) that was almost suppressed by 500 µM 4-AP (0.5 ± 0.2 pA, n = 10). In approximately 30% of MβCD-tested patches, 4-AP unmasked large conductance channels (≈135 pS) resembling maxi-anion channels (22). These channels were not observed under control conditions.

A high channel activity was recorded in AAM expressing hKv1.5-EGFP channels (mean current: 2.3 ± 0.8 pA, n = 11) (Fig. 2*B*). Following MβCD application, channel activity increased at nearly the same time as in native cells (6–10 min), reached a high value (47.5 ± 7.2 pA, $n = 11$) and was suppressed by 4-AP. The enhanced channel activity is mainly due to a marked increase in number of unitary current levels as illustrated by the amplitude histogram (Fig. S1). Interestingly, during overexpression experiments, large conductance channel openings were not detected. These results indicate that cholesterol depletion increases the surface density of Kv1.5 channels.

Cholesterol Depletion Reduces the Mobile Fraction of Kv1.5 Channels. Next, we examined whether cholesterol depletion can modify Kv1.5 channel distribution. Because the mobility of channels depends on their compartmentalization (13), we first investigated the effect of cholesterol depletion on Kv1.5 channel mobility using the FRAP technique. Randomly selected regions of interest (ROI) at the edge of myocytes were photobleached, and fluorescence recovery within the ROI was monitored over the time by scanning until steady-state was reached (Fig. 3). The mobile fraction was greatly reduced in

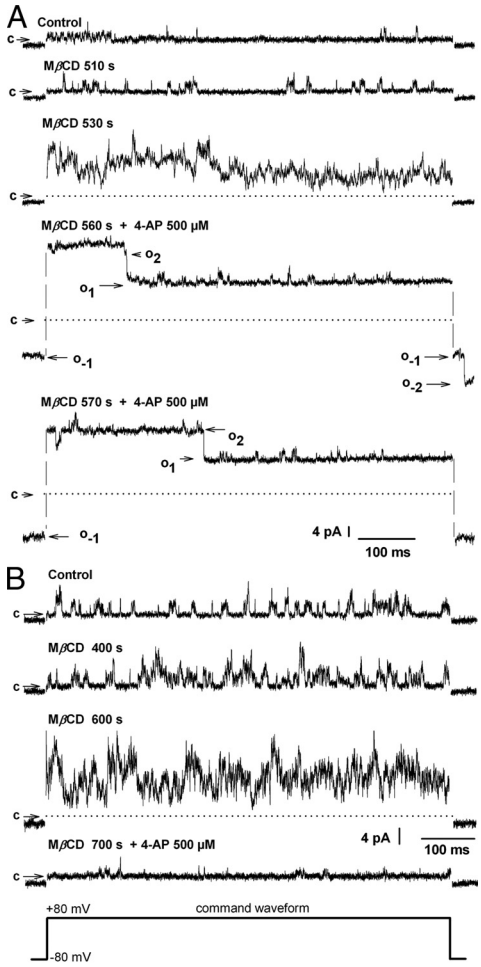

Fig. 2. Cholesterol depletion increases the number of channels in the plasma membrane of atrial myocytes. Sample traces from cell-attached membrane showing that MβCD increases single-channel activity in freshly isolated (*A*) and hKv1.5-EGFP-expressing myocytes (*B*). Note that under 4-AP the activity of large conductance channels was unmasked (*A*). o_{-n}, downward open, level n; o_n, upward open, level n; c, closed level. Arrows and dotted lines indicate the closed state.

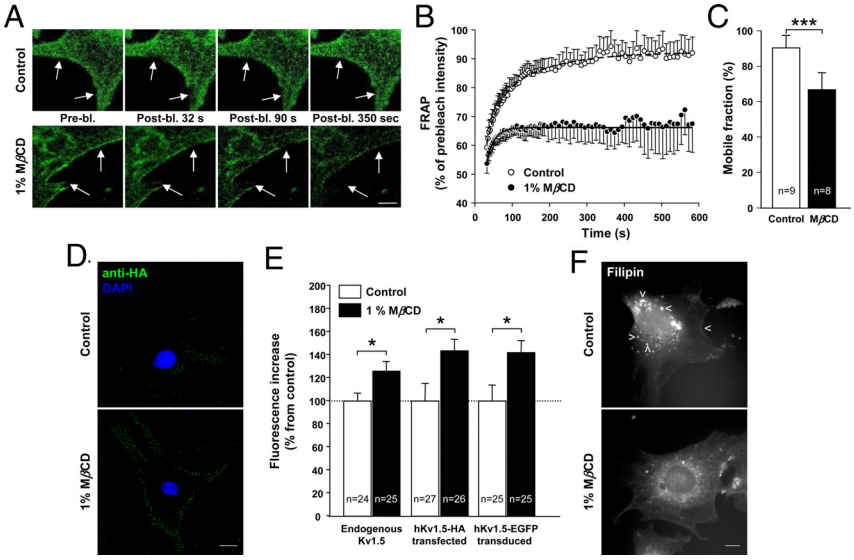

Fig. 3. Cholesterol depletion reduces the mobility and redistributes Kv1.5 channels in atrial myocytes. (*A*) Sequential images from FRAP experiments obtained in control prebleach (prebl.) and at various times postbleach (postbl.) in hKv1.5-EGFP expressing myocytes treated or not with 1% MβCD for 10 min. Arrows indicate representatives ROI. Bar, 10 μm. (*B*) Kinetics of hKv1.5 fluorescence recovery in control and MβCD conditions. (*C*) Mobile fraction (M_f) measured at the end of the FRAP experiment. (*D*) Deconvoluted images of HA surface staining in cultured AAM treated or not with 1% MβCD. (*E*) Fluorescence intensity of endogenous Kv1.5 channels, hKv1.5-HA-transfected, and hKv1.5-EGFP-transduced AAM. (*F*) Filipin-stained cells without and with MβCD-treatment.

MβCD-treated AAM (control: % of M_f = 91.5 ± 7.2, n = 9 vs. MβCD: % of M_f = 67.9 ± 9.2, n = 8, $P < 0.001$) (Fig. 3*C*). In control cells, the fluorescence recovery was best fitted by a double exponential function with a τ fast of 29 ± 2.6 s and τ slow of 137 ± 9.3 s (n = 9) (Fig. 3*B*). Only a fast component could be extracted from MβCD-treated AAM at 21 ± 2.2 s postbleach (n = 8).

In AAM stained with an anti-Kv1.5 antibody, the fluorescence related to endogenous channels increased by 26 ± 8.5% after MβCD-treatment (Fig. 3 *E* and $P < 0.05$). Then, myocytes were transfected with a plasmid encoding for hKv1.5 tagged with the hemagglutinin (HA) inserted into an extracellular loop to permit the detection of channels present at the cell surface. Following MβCD application, HA-staining increased by 43.64 ± 9.97% ($P < 0.05$) (Fig. 3 *D* and *E*). MβCD treatment also induced a 41.8 ± 10.6% increase of the GFP fluorescence ($P < 0.05$) at the cell periphery of hKv1.5-EGFP-transduced AAM (Fig. 3*E*). The effectiveness of 10 min of MβCD application to deplete cholesterol was checked using filipin, a marker of cholesterol enriched domains (Fig. 3*F*). In control myocytes, filipin was organized in intracellular dense spots and at the level of the plasma membrane. After short MβCD applications, only a faint peripheral staining remained.

Taken together, these results suggest that cholesterol depletion modified the mobility and compartmentalization of Kv1.5 channels in myocytes.

Cholesterol Modulates the Density of Functional Kv1.5 Channels via Rab11. Different steps in Kv1.5 channel trafficking were then investigated. First, exocytosis of channels by SNARE-mediated fusion processes was addressed using the inhibitor *N*-ethylmaleimide (NEM) in hKv1.5-EGFP-transduced AAM. In all cells recorded, 10 min dialysis of 250 μM NEM via the patch pipette prevented the IKur increase (Fig. 4*A*).

Second, the involvement of the secretory pathway in the MβCD-effect was explored using brefeldin A (BFA) to prevent the formation of coatamers at the Golgi exit. In all myocytes tested, 2 to 6 h incubation with 5 μM BFA did not preclude the MβCD effect on I_{Kur} (Fig. 4*B*).

As a general approach to test the involvement of Rab-GTPases in the MβCD effect, 500 μM GTPγS, a nonhydrolyzable form of GTP, was dialyzed in AAM via the patch pipette. After 10 min of dialysis, MβCD had no effect on I_{Kur} (Fig. 4*C*). To identify which Rab-GTPases were involved in the MβCD effect on Kv1.5 channels, AAM were transfected with constitutively active (CA) or dominant negative (DN) mutants of Rab proteins (Fig. 5). In AAM transfected with either CA or DN Rab4 constructs, there was no difference in the density of outward currents (Rab4 CA: 10.8 ± 5.5 pA/pF, n = 6 vs. Rab4 DN: 12.1 ± 5.6 pA/pF, n = 9) (Fig. 5*B*), and 1% MβCD exerted a stimulatory effect on I_{Kur} in both CA and DN-transfected AAM (Rab4 CA: 42.3 ± 6.7 pA/pF, n = 6 vs. Rab4 DN: 64.8 ± 17.3 pA/pF, n = 9). Interestingly, Rab11 CA induced a slight but significant decrease in I_{Kur} in comparison to Rab11 DN (CA: 6.1 ± 1.3 pA/pF, n = 7 vs. DN: 15.6 ± 2.5 pA/pF, n = 9, $P < 0.01$). Whereas MβCD still increased I_{Kur} in Rab11 CA-transfected AAM, it no longer had an effect in cells expressing Rab11 DN (Rab11 CA: 34.0 ± 3.9 pA/pF, n = 7; Rab11 DN: 17.0 ± 8.6 pA/pF, n = 9) (Fig. 5*C*). These results indicated clearly the involvement of Rab11-associated RE in the effect of cholesterol depletion on Kv1.5 channels.

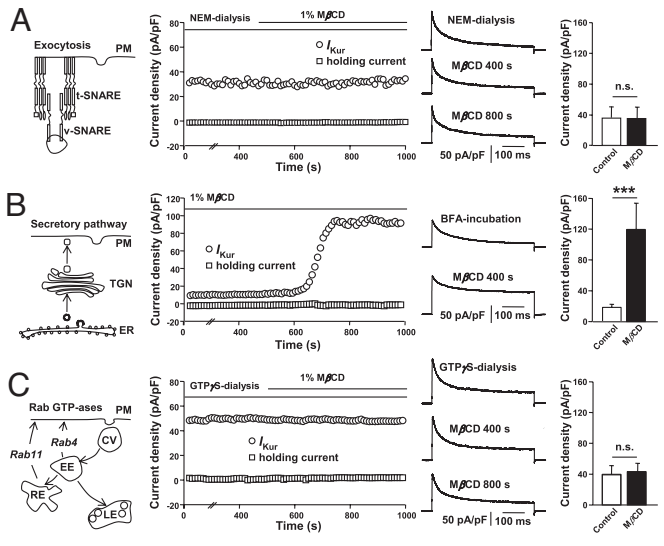

Fig. 4. The effect of MβCD on I_{Kur} involves Kv channel exocytosis. From left to right: diagram indicating the trafficking steps studied, the time course of I_{Kur} and holding current, I_{Kur} traces and statistical analysis of control and MβCD. (*A*) Effect of the SNARE inhibitor N-ethylmaleimide (NEM, 250 μM) applied intracellularly for 10 min before MβCD perfusion (n = 5). (*B*) Effect of a 6 h incubation with 5 μM brefeldin A (BFA), an inhibitor of Golgi exit, before patch-clamp experiment (n = 5). (*C*) Effect of 10-min dialysis with a nonhydrolyzable GTP analogue, GTP-γ-S (500 μM) before MβCD perfusion (n = 5). TGN, transGolgi Network; ER, endoplasmic reticulum; CV, coated vesicle; LE, late endosome.

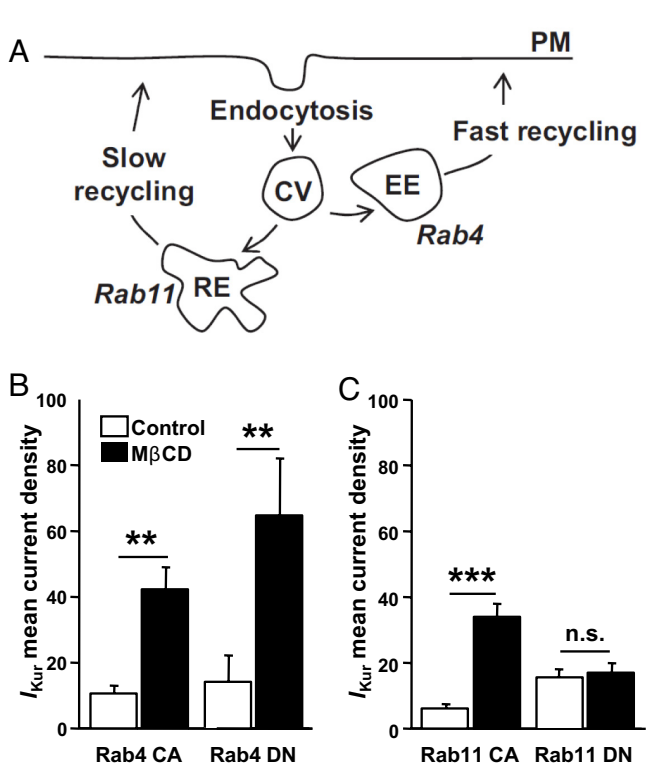

Fig. 5. The Rab11 GTP-ase is responsible for the stimulatory effect of MβCD on I_{Kur} in atrial myocytes. (*A*) Picture of the 2 compartments associated to specific Rab proteins. Current densities obtained in control Tyrode and following 1% MβCD application in myocytes transfected with constitutively active (CA) or dominant negative (DN) Rab4 (*B*) or Rab11 (*C*) constructs.

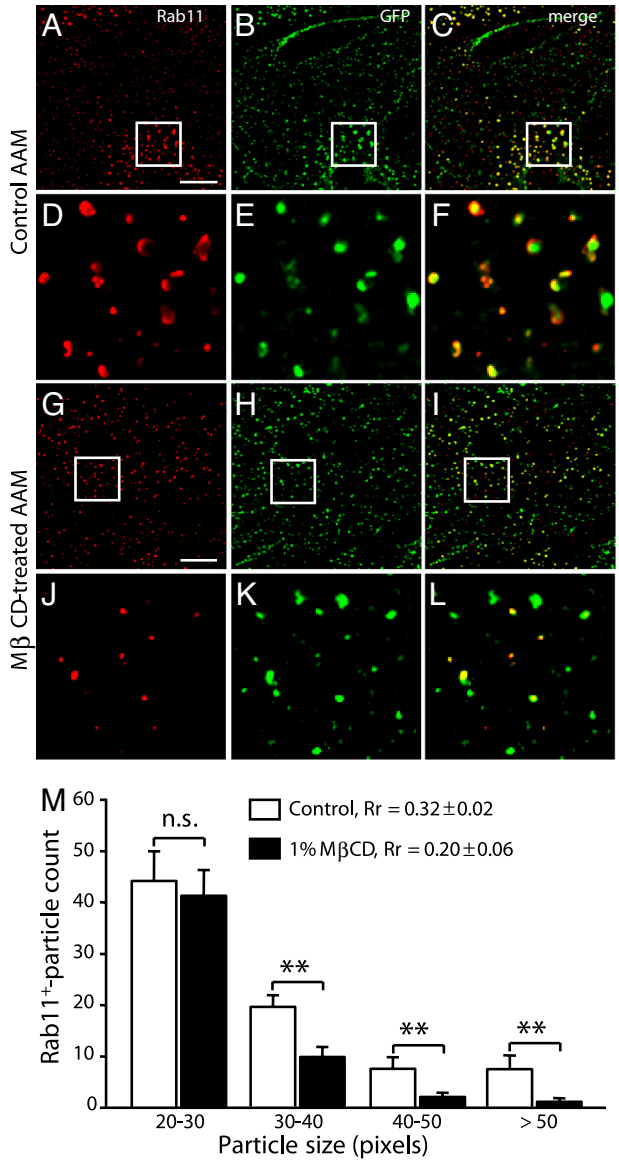

Fig. 6. Rab11 and hKv1.5 channel association is suppressed by cholesterol depletion. (*A–L*) Deconvolution images of Rab11 (red) and GFP (green) staining in control (*A–F*) and MβCD treated-(*G–L*) myocytes. Panels (*D–F*) and (*J–L*) are enlarged single planes from the squared regions of the corresponding z-stacks in (*A–C*) and (*G–I*). Note that the size of double-stained particles was drastically diminished following MβCD-treatment. (*M*) Distribution of Rab11-positive particles in function of their size in control ($n = 6$) and MβCD-treated AAM ($n = 10$). (Scale bar, 10 μm in *A–C* and *G–I*; 2 μm in *D–F* and *J–L*; 1 pixel, 0.1 μm.)

A Fraction of the Kv1.5 Channels Are Localized in the Rab11-associated Endosome in Myocytes. The interaction between Kv1.5 channels and Rab11 proteins was further investigated by studying first their interaction using a coimmunoprecipitation assay. In hKv1.5-EGFP-expressing myocytes, the anti-GFP antibody precipitated a large 100-kDa band (molecular weight of Kv1.5-EGFP) (Fig. S2). Probing the membrane with the anti-Rab11 antibody revealed a coprecipitated band at ≈25 kDa, the molecular weight of the Rab protein. Localization of hKv1.5-EGFP and Rab11 was studied using 3-dimensional microscopy. Fig. 6 *A–L* show deconvolution images of myocytes double stained with anti-GFP and anti-Rab11 antibodies. Rab11 and Kv1.5 channels distributed throughout the cell and formed particles of different sizes, with a strong expression in the perinuclear region (Fig. 6 *A–C* and *G–I*). Enlargement of single focal planes from Fig. 6 *A–C* clearly demonstrated the association of Rab11 and GFP-positive vesicles, the Rab11 fluorescence tightly surrounding the GFP staining. In MβCD-treated cells (Fig. 6 *J–L*), this association was reduced (Pearson coefficient in control: 0.32 ± 0.02, $n = 6$ vs. in MβCD-treated: 0.20 ± 0.05, $n = 10$). Additionally, the size of Rab11-positive dots was drastically reduced in MβCD-treated AAM: big-sized particles diminished following MβCD treatment (Fig. 6*M*). These results indicate that Kv1.5 channels and Rab11 are associated in myocytes; depleting cholesterol causes the dissociation of Kv1.5 channels and Rab11-associated vesicles.

Discussion

This study provides evidence that in adult atrial myocytes, the recycling endosome can constitute a storage compartment of Kv1.5 channels readily available for recruitment into the plasma membrane upon cholesterol depletion.

We found that following MβCD application, more active Kv1.5 channels are inserted in the plasma membrane of myocytes as evidenced by the direct recording of single-channel activity. The effect of MβCD on the whole-cell outward potassium current likely results from this increase in Kv1.5 channel density given the high 4-AP sensitivity of the MβCD-current and the concomitant time course of drug effect on whole-cell currents and single-channel activity. As well, MβCD-activated current was no longer observed when the molecule was saturated with cholesterol, and since LDL had an opposite effect on cardiac potassium currents, the MβCD effect on current appears mainly related to its capacity to deplete membrane cholesterol. The redistribution of filipin staining following 10 min MβCD-application indicates that short treatment is sufficient to induce cholesterol depletion in cardiomyocytes.

Membrane cholesterol regulates the surface expression of several ion channels including K_{ir}, volume-regulated anion currents

(VRAC) or CFTR channels (11, 21, 23, 24). Interestingly, in the present study activity of a large conductance channel was also often recorded upon long-lasting MβCD application. These unitary currents had the properties of maxi-anion channels which are not present normally in the plasma membrane (22). The absence of these maxi anion channels in myocytes overexpressing Kv1.5 channels could indicate a saturation of the membrane by an excessive amount of exogenous channels. Altogether, these results point to a common pathway modulated by cholesterol for the recruitment of cardiac ion channels into the plasma membrane. However, the observation that cholesterol depletion significantly decreased the fast component of I_{to} suggests that distinct mechanisms regulate the functional expression of Kv4.x and Kv1.5 channels as reported for Kv2.1 and Kv1.4 channels in cardiomyocytes (25).

In cardiomyocytes as in other cell types, it has been shown that a fraction of Kv channels is mobile and could represent a submembrane vesicular compartment while immobile channels could be linked to the cytoskeleton and organized in protein complexes (13). In the same line, the anchoring protein SAP97 that binds Kv1.5 channels to the cytoskeleton (26) reduces the mobility of Kv1.5 channels resulting in increased I_{Kur} (27). Thus, FRAP experiments showing that cholesterol depletion immobilizes a fraction of Kv1.5 channels suggests a redistribution of protein from a mobile compartment to anchoring domains (28). This is supported by the fluorescence signal increase of endogenous, EGFP- or HA-tagged Kv1.5 channels at the plasma membrane of MβCD-treated myocytes. However, the discrepancy between the increase in activity and surface expression of channels suggests that only some of the Kv1.5 channels visualized at the level of the plasma membrane are functional, as has been reported for Kv2.1 channels (29).

Undoubtedly, the 6–10 min necessary to observe the MβCD effect on I_{Kur} is too brief to support new synthesis of channels. The ineffectiveness of BFA, which disrupts the Golgi complex (30) to counteract the MβCD effect eliminates a major contribution of the secretion pathway. Soluble *N*-ethylmaleimide (NEM)-sensitive factor attachment receptor (SNARE) proteins are represented by a superfamily of small membrane-associated proteins that mediate membrane fusion. Suppression of the MβCD effect on I_{Kur} following NEM treatment therefore strongly suggests that cholesterol regulates exocytosis of Kv1.5 channels. A likely explanation is that the effects of cholesterol on I_{Kur} depend on Kv1.5-containing trafficking vesicles from the retrograde pathway, that is, from the EE or RE. Here, we provide strong evidence for the involvement of Rab11-associated RE in the effect of cholesterol on Kv1.5 channels. First, Rab11 was highly expressed in myocytes and precipitated Kv1.5 channels. Second, transfection of myocytes with a DN and not the CA form of Rab11 completely prevented the MβCD effect on I_{Kur} while both Rab4 DN and Rab4 CA were ineffective. Interestingly, overexpression of Rab11 CA also reduced basal I_{Kur}, suggesting that the RE is a constitutive route of Kv1.5 channels trafficking. Thus, enhancing RE function induces the accumulation of Kv1.5 channels in this storage compartment and consequently, prevents recycling to the plasma membrane. Third, high spatial resolution 3D microscopy reveals that Rab11 proteins surround large spots of EGFP-tagged Kv1.5 in the perinuclear region of control AAM. Following MβCD treatment, the size of Rab11-positive particles and their colocalization with Kv1.5 channels were reduced. One likely explanation is that cholesterol depletion, in addition to causing a redistribution of cholesterol in membranes, enhances the insertion of Kv1.5 channels in the plasma membrane by favoring the release of channels from the RE, as shown by the dissociation of the two proteins.

All these findings are in good agreement with previous studies demonstrating a role for Rab11 in the regulation of ion channel density in the cardiac muscle and/or in cell lines. For instance, a Rab11-mediated recycling has been reported for the glucose transporter GluT4 (31), the KCNQ1/KCNE1 potassium channel (10), β-adrenergic receptors (32), as well as for the Kv1.5 channels expressed in cell lines (8, 9).

Cholesterol regulates different steps in trafficking of ion channels or receptors. For instance, lowering cholesterol with MβCD can either alter endocytosis (15, 18, 19), redistribute proteins into membrane subdomains (33), or reduce endosomal mobility (16). Cholesterol can also modulate recycling processes (17, 19). First, by interacting with sterol-binding domains of proteins in the recycling compartment, cholesterol could control interactions with the plasma membrane and the subsequent insertion of ion channels. Recently, an interaction between cholesterol and podocin has been reported in the recruitment of TRPC channels into the plasma membrane (34). Second, membrane composition could account for their sensitivity to cholesterol depletion (35, 36). The RE, enriched in cholesterol compared to the EE or the plasma membrane, is quick to reorganize following changes in cholesterol (37). Finally, modifications of cholesterol content, through their effects on membrane properties, could also alter vesicle trafficking and fusion processes. For instance, redistribution of the NPC1 protein following changes in cholesterol content was attributed to trafficking alterations in Niemann-Pick type C disease (38). Interestingly, the kinetic of NPC1L1 trafficking between RE and plasma membrane is modulated by cholesterol content in hepatoma cells (39).

Physiological Significance. Recruitment of channels into the plasma membrane from submembrane vesicle pools has been described in other excitable cells and is a major mechanism for the fine tuning and adaptation to extracellular stimuli of the electrical excitability. This is well known for neurotransmission and for instance, the synaptic recruitment of AMPAR or Kv channels during long-term potentiation (40, 41). The adaptation of cardiac electrical properties to stress or angiotensin II stimulation could also depend on the recruitment from Rab11-associated vesicles of delayed rectifier (10) or pacemaker (42) channels. Changes in cholesterol content, for instance following lipid-lowering treatment, could represent another condition that stimulates the turnover and recruitment of Kv channels in myocytes. Interestingly there are already reports that chronic modification of lipid composition of cardiac membranes are associated with posttranscriptional changes in the surface density of Kv channels which might involve trafficking processes (5, 43). Further studies aiming to determine how recruitment of Kv channels from these submembrane pools contributes to normal and pathological cardiac functions are warranted.

Materials and Methods

Myocyte Cultures. AAM were isolated from rat atria as described previously (12) and cultured for 3 to 5 days before patch-clamp and imaging experiments. Neonatal rat myocytes (NRC) were isolated from whole hearts (12) and used for co-IP experiments. Myocytes were cultured either in standard condition (37°C, 5% CO_2) or in low CO_2 (37°C, 1%) for plasmid transfection purpose using a liposome-based approach (44).

Adenovirus Infections and Plasmid Transfections. Human (h) Kv1.5 channel cDNA with the EGFP sequence in C-terminal was subcloned in adenovirus and was used at 3.2 10^5 pi/mL (11). The DN and CA constructs of Rab4 (S22N and Q67L) or Rab11 (S25N and Q70L) were cloned in pEGFP-C1 vector. pcDNA3-Kv1.5-HA was generated by inserting the HA tag into hKv1.5 extracellular loop between residues 307 and 308 (9).

Immunofluorescence and 3D Microscopy. Images were acquired with a cooled CoolSnap camera (Roper Scientific) on an Olympus epifluorescent microscope (60×, UPlanSApo, 0.17). Images were processed and analyzed using Metamorph (Molecular Devices) supplemented with the 3D-deconvolution module. For each sample, 2–4 consecutive z-images (sectioning step: 0.2 μm) were thresholded to similar levels. Filipin staining was achieved on fixed cells preincubated with 1.5 mg/mL glycine in PBS for 30 min, then incubated with filipin (250 μg/mL) for 1 h at RT before epifluorescence microscopy. Surface Kv1.5 fluorescence was evaluated using a mouse anti-HA antibody (Roche) on fixed nonpermeabilized hKv1.5-HA-transfected cells. Kv1.5 fluorescence was also measured at the cell periphery of cells transduced with hKv1.5-EGFP adenovirus (rabbit anti-GFP, Torrey Pines).

Fluorescence analysis was performed for each individual z-images using ImageJ software.

FRAP Experiments and Confocal Microscopy. FRAP studies were performed on hKv1.5-EGFP-transduced AAM using a Leica SP2 confocal microscope (63×, 1.4 NA), at 37°C. Squared ROI were photobleached by scanning with the 488-nm line of Argon laser (100% transmission). Pre- and postbleach images were acquired at 512 × 512 resolution (laser: 2% transmission). Postbleach images were acquired every 3 s for 1 min, then every 5 s for 2 min and every 10 s for 7 min. Correction for overall photobleaching was performed by subtracting fluorescence intensity in nonbleached ROI from all intensity data points. Average fluorescence intensity within ROI was then normalized to prebleach intensity for each time point and plotted as a function of time. Recovery kinetic and mobile fractions were calculated as described previously (27). Fluorescence intensity at the cell periphery was measured from Nomarski and confocal images of fixed native AAM stained with an anti-Kv1.5 antibody (Alomone Labs) using ImageJ.

Coimmunoprecipitation and Western Blotting. Proteins were extracted from hKv1.5-EGFP-transduced neonatal rat myocytes (44), precleared with protein G-Sepharose beads (Sigma) and incubated overnight at 4°C with 2 μg of antibodies for immunoprecipitation. Proteins were separated on 10% polyacrylamide-SDS gels and transferred to polyvinylidene difluoride membranes (Amersham). Western blotting was performed with rabbit and mouse anti-GFP (Torrey Pines and Roche, respectively) and mouse anti-Rab11 (BD Transduction).

Patch Clamp. Currents were recorded using borosilicate glass pipettes (resistance 1.5–2 MΩ and 10–15 MΩ for whole-cell and single-channel recordings, respectively) with a patch-clamp amplifier (Axoclamp 200B; Axon Instrument) (27). Outward currents were activated using test pulses (750 ms) to + 60 mV (whole-cell) or + 80 mV (single-channel) from a holding potential of −80 mV at a frequency of 0.1 Hz. All experiments were conducted at RT.

Drugs. MβCD (1%) and 4-aminopyridine (4-AP, 500 μmol/L) were prepared in the perfusing Tyrode solution. *N*-ethylmaleimide (250 μmol), and GTPγS (500 μmol/L) were diluted in the pipette solution and dialysed to the cells. BFA (5 μmol/L) was diluted in the culture medium and incubated for 6 h before recordings. For experiments with LDL, AAM were serum-starved for 1 night and incubated with 50 μg/mL LDL for 24 h. LDL was kindly provided by S. Karabina (UMRS937). All chemicals were purchased from Sigma.

Data Analysis. Data are expressed as means ± SEM. Statistical significance was estimated with Student's *t* tests or ANOVA, as appropriate. *P* values of <0.05 were considered significant. *: $P < 0.05$, **: $P < 0.01$ and ***: $P < 0.001$.

ACKNOWLEDGMENTS. We thank Agence Nationale de la Recherche (ANR-05-PCOD-006–01) for their financial support. Saïd El-Haou is the recipient of a fellowship from the Association Française contre les Myopathies.

1. Lundbaek JA, Birn P, Girshman J, Hansen AJ, Andersen OS (1996) Membrane stiffness and channel function. *Biochemistry* 35:3825–3830.
2. Oliver D, *et al.* (2004) Functional conversion between A-type and delayed rectifier K+ channels by membrane lipids. *Science* 304:265–270.
3. Epshtein Y, *et al.* (2009) Identification of a C-terminus domain critical for the sensitivity of Kir2.1 to cholesterol. *Proc Natl Acad Sci USA* 106:8055–8060.
4. Savelieva I, Camm J (2008) Statins and polyunsaturated fatty acids for treatment of atrial fibrillation. *Nat Clin Pract Cardiovasc Med* 5:30–41.
5. Tamargo J, *et al.* (2007) Lipid-lowering therapy with statins, a new approach to antiarrhythmic therapy. *Pharmacol Ther* 114:107–126.
6. Loewen ME, *et al.* (2009) Shared requirement for dynein function and intact microtubule cytoskeleton for normal surface expression of cardiac potassium channels. *Am J Physiol Heart Circ Physiol* 296:H71–83.
7. Choi WS, *et al.* (2005) Kv1.5 surface expression is modulated by retrograde trafficking of newly endocytosed channels by the dynein motor. *Circ Res* 97:363–371.
8. McEwen DP, *et al.* (2007) Rab-GTPase-dependent endocytic recycling of Kv1.5 in atrial myocytes. *J Biol Chem* 282:29612–29620.
9. Zadeh AD, *et al.* (2008) Internalized Kv1.5 traffics via Rab-dependent pathways. *J Physiol* 586:4793–4813.
10. Seebohm G, *et al.* (2007) Regulation of endocytic recycling of KCNQ1/KCNE1 potassium channels. *Circ Res* 100:686–692.
11. Romanenko VG, Rothblat GH, Levitan I (2002) Modulation of endothelial inward-rectifier K+ current by optical isomers of cholesterol. *Biophys J* 83:3211–3222.
12. Abi-Char J, *et al.* (2007) Membrane cholesterol modulates Kv1.5 potassium channel distribution and function in rat cardiomyocytes. *J Physiol* 582:1205–1217.
13. O'Connell KM, Tamkun MM (2005) Targeting of voltage-gated potassium channel isoforms to distinct cell surface microdomains. *J Cell Sci* 118:2155–2166.
14. Fedida D, *et al.* (1993) Identity of a novel delayed rectifier current from human heart with a cloned K+ channel current. *Circ Res* 73:210–216.
15. Borroni V, *et al.* (2007) Cholesterol depletion activates rapid internalization of submicron-sized acetylcholine receptor domains at the cell membrane. *Mol Membr Biol* 24:1–15.
16. Chen H, Yang J, Low PS, Cheng JX (2008) Cholesterol level regulates endosome motility via Rab proteins. *Biophys J* 94:1508–1520.
17. Choudhury A, Sharma DK, Marks DL, Pagano RE (2004) Elevated endosomal cholesterol levels in Niemann-Pick cells inhibit rab4 and perturb membrane recycling. *Mol Biol Cell* 15:4500–4511.
18. Subtil A, *et al.* (1999) Acute cholesterol depletion inhibits clathrin-coated pit budding. *Proc Natl Acad Sci USA* 96:6775–6780.
19. Wasser CR, Ertunc M, Liu X, Kavalali ET (2007) Cholesterol-dependent balance between evoked and spontaneous synaptic vesicle recycling. *J Physiol* 579:413–429.
20. Boyle WA, Nerbonne JM (1992) Two functionally distinct 4-aminopyridine-sensitive outward K+ currents in rat atrial myocytes. *J Gen Physiol* 100:1041–1067.
21. Fang Y, *et al.* (2006) Hypercholesterolemia suppresses inwardly rectifying K+ channels in aortic endothelium in vitro and in vivo. *Circ Res* 98:1064–1071.
22. Coulombe A, Coraboeuf E (1992) Large-conductance chloride channels of new-born rat cardiac myocytes are activated by hypotonic media. *Pflugers Arch* 422:143–150.
23. Guo J, *et al.* (2007) Identification of IKr and its trafficking disruption induced by probucol in cultured neonatal rat cardiomyocytes. *J Pharmacol Exp Ther* 321:911–920.
24. Levitan I, Christian AE, Tulenko TN, Rothblat GH (2000) Membrane cholesterol content modulates activation of volume-regulated anion current in bovine endothelial cells. *J Gen Physiol* 115:405–416.
25. O'Connell KM, Whitesell JD, Tamkun MM (2008) Localization and mobility of the delayed-rectifer K+ channel Kv2.1 in adult cardiomyocytes. *Am J Physiol Heart Circ Physiol* 294:H229–237.
26. Eldstrom J, Choi WS, Steele DF, Fedida D SAP97 increases Kv1.5 currents through an indirect N-terminal mechanism. *FEBS Lett* 547:205–211, 2003.
27. Abi-Char J, *et al.* (2008) The anchoring protein SAP97 retains Kv1.5 channels in the plasma membrane of cardiac myocytes. *Am J Physiol Heart Circ Physiol* 294:H1851–1861.
28. Feder TJ, Brust-Mascher I, Slattery JP, Baird B, Webb WW (1996) Constrained diffusion or immobile fraction on cell surfaces: a new interpretation. *Biophys J* 70(6):2767–2773.
29. Benndorf K, Koopmann R, Lorra C, Pongs O (1994) Gating and conductance properties of a human delayed rectifier K+ channel expressed in frog oocytes. *J Physiol* 477:1–14.
30. Sciaky N, *et al.* (1997) Golgi tubule traffic and the effects of brefeldin A visualized in living cells. *J Cell Biol* 139:1137–1155.
31. Uhlig M, Passlack W, Eckel J (2005) Functional role of Rab11 in GLUT4 trafficking in cardiomyocytes. *Mol Cell Endocrinol* 235:1–9.
32. Filipeanu CM, *et al.* (2006) Enhancement of the recycling and activation of beta-adrenergic receptor by Rab4 GTPase in cardiac myocytes. *J Biol Chem* 281:11097–11103.
33. Tikku S, *et al.* (2007) Relationship between Kir2.1/Kir2.3 activity and their distributions between cholesterol-rich and cholesterol-poor membrane domains. *Am J Physiol Cell Physiol* 293:C440–450.
34. Huber TB, *et al.* (2006) Podocin and MEC-2 bind cholesterol to regulate the activity of associated ion channels. *Proc Natl Acad Sci USA* 103:17079–17086.
35. Lange Y, Ye J, Rigney M, Steck TL (1999) Regulation of endoplasmic reticulum cholesterol by plasma membrane cholesterol. *J Lipid Res* 40:2264–2270.
36. Keller P, Simons K (1998) Cholesterol is required for surface transport of influenza virus hemagglutinin. *J Cell Biol* 140:1357–1367.
37. Hao M, Mukherjee S, Sun Y, Maxfield FR (2004) Effects of cholesterol depletion and increased lipid unsaturation on the properties of endocytic membranes. *J Biol Chem* 279:14171–14178.
38. Kobayashi T, *et al.* (1999) Late endosomal membranes rich in lysobisphosphatidic acid regulate cholesterol transport. *Nat Cell Biol* 1:113–118.
39. Petersen NH, Faergeman NJ, Yu L, Wustner D (2008) Kinetic imaging of NPC1L1 and sterol trafficking between plasma membrane and recycling endosomes in hepatoma cells. *J Lipid Res* 49:2023–2037.
40. Grosshans DR, Clayton DA, Coultrap SJ, Browning MD (2002) LTP leads to rapid surface expression of NMDA but not AMPA receptors in adult rat CA1. *Nat Neurosci* 5:27–33.
41. Kim J, Jung SC, Clemens AM, Petralia RS, Hoffman DA (2007) Regulation of dendritic excitability by activity-dependent trafficking of the A-type K+ channel subunit Kv4.2 in hippocampal neurons. *Neuron* 54:933–947.
42. Hardel N, Harmel N, Zolles G, Fakler B, Klocker N (2008) Recycling endosomes supply cardiac pacemaker channels for regulated surface expression. *Cardiovasc Res* 79:52–60.
43. Koshida S, *et al.* (2009) Stabilizing effects of eicosapentaenoic acid on Kv1.5 channel protein expressed in mammalian cells. *Eur J Pharmacol* 604:93–102.
44. El-Haou S, *et al.* (2009) Kv4 potassium channels form a tripartite complex with the anchoring protein SAP97 and CaMKII in cardiac myocytes. *Circ Res* 104:758–769.